

Synthesis and Application Properties of Fluorinated Aromatic Copolymers

Haohua Ye,^{1,2} Zhanxiong Li,^{1,2} Guoqiang Chen^{1,2}

¹National Engineering Laboratory for Modern Silk, Suzhou University, Jiangsu 215123, China

²College of Textile and Clothing Engineering, Suzhou University, Jiangsu 215006, China

Correspondence to: G.Q. Chen (E-mail: chenguoqiang@suda.edu.cn)

ABSTRACT: Aromatic monomers with different fluorine concentrations and structural distribution patterns were synthesized. A series of copolymers based on methyl methacrylate, acrylate, and perfluorooctylalkyl acrylate were prepared by emulsion polymerization and were subsequently used as functional coatings to prepare water- and oil-repellent cotton fabrics. The composition and structure of the outmost layer of the treated cotton surface were analyzed. A strong surface segregation of fluorinated segments was found for the treated samples, as shown by X-ray photoelectron spectroscopy analysis. The basis for an in-depth appreciation of the relationship between the molecular structure of the monomers and the properties of corresponding copolymer-treated materials was provided (especially with regarding to their hydrophobic and oleophobic properties). The wetting characteristics of the fluorinated copolymers were found to be dependent on the density (number of side chains per constitutional repeat unit) and regularity of the fluorinated side chains. © 2013 Wiley Periodicals, Inc. *J. Appl. Polym. Sci.* 130: 4410–4418, 2013

KEYWORDS: coatings; copolymers; emulsion polymerization; textiles

Received 18 February 2013; accepted 28 April 2013; Published online 22 July 2013

DOI: 10.1002/app.39474

INTRODUCTION

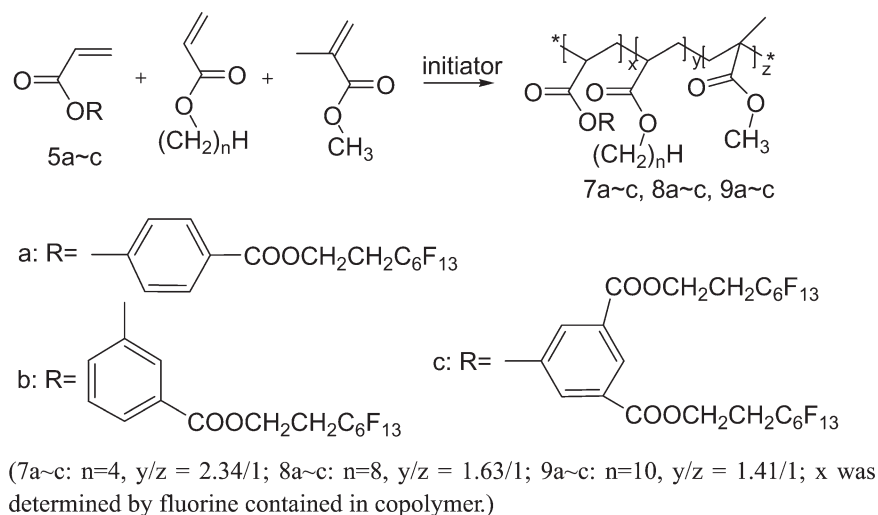
Fluorinated copolymers have attracted much interest for their wide applications in lowering surface energy.^{1–4} Polymers containing long-chain fluoroalkyl groups have excellent water and oil repellency, although recently they have been found to cause a series of problems, such as bioaccumulation and environmental damage.^{5–7} Studies now are mainly focusing on the exploration of environmentally friendly materials, such as polymers with short perfluorocarbon chains (repeat units of $\text{CF}_2 < 8$) for their easy degradable properties.^{8–10}

The hydrophobic and oleophobic properties of fluorinated polymers depend on the orientation of the fluorinated chains.¹¹ Optimum water and oil repellent property can be obtained only if the fluorinated chain is vertical with the substrate surface. Generally, the linkage structure in the fluorinated acrylate molecule is considered to be very important to the stability of the monomer as is the orientation of the fluorinated side chains in the ultimate polymers. In this study, three monomers containing aromatic rings were synthesized. We believed that the conjugate-plane rigid frame of the aromatic ring might be beneficial to the regular arrangement of the side chains onto the surface and would exhibit better surface properties, such as better water- and oil-repellent properties. It was reported that closely packed clusters of two or more fluorinated groups in monomer

could increase the concentration of fluorine in the outmost surface of corresponding copolymer and finally increase the hydrophobicity and oleophobicity of resulting film.^{12–14} To increase the concentration of fluoroalkyl chains in the outmost surface of polymer, two fluoroalkyl groups were introduced into the molecule of the monomer 5-acryloyloxyisophthalic acid bis(tetrahydroperfluorooctanol) ester (FIP or 5c).

Fluorinated *p*-acryloyloxybenzoates had been reported in some studies, and their polymers have been found to exhibit a high, durable water/oil repellency.^{15,16} In previous studies, tetrahydroperfluorooctanol *p*-hydroxybenzoate were prepared with tetrahydroperfluorooctanol as a reactor and solvent in a depressurized system. However, the use of tetrahydroperfluorooctanol as a solvent was uneconomical; also, the depressurized reaction system was relatively complicated. Here, the reaction was carried in an atmospheric pressure system; toluene was used as a water-carrying agent to separate the water from the reactants and accelerate the reaction. The preparation of fluorinated *m*-acryloyloxybenzoate or fluorinated 5-acryloyloxyisophthalic acid bisester has seldom been reported to this point. In this study, we aimed to partially fill this gap. In this study, three aromatic monomers were synthesized.

Emulsion polymerization is extensively used for the preparation of fluorinated acrylate copolymers to exclude environmentally



Scheme 3. Copolymerization of the fluorinated monomers.

water collected in the Dean–Stark tube were taken every 10 min from the time that the water was removed by azeotropic distillation with toluene. The reaction was kept for about 8 h until no water was yielded. After it was cooled to room temperature, the solvent was removed under reduced pressure. The solid precipitated from the liquid was subsequently washed with a 5% NaOH solution, cold water, hot water, and dilute hydrochloric acid. After recrystallization, the pure **3a** was obtained.

The compound tetrahydroperfluorooctanol *m*-hydroxybenzoate (**3b**) was prepared under the same conditions used for **3a** by the reaction of 3-hydroxybenzoic acid with 1,1,2,2-tetrahydroperfluorooctanol.

Synthesis of tetrahydroperfluorooctanol *p*-acryloyloxybenzoate (FPB or 5a). **3a** (13.81 g, 0.10 mol), dichloromethane (40 mL), and TEA (12.13 g, 0.12 mol) were placed in a flask. Acryloyl chloride (10.86 g, 0.12 mol) was added dropwise within 2 h at 0°C and stirred at room temperature for additional 12 h. The resulting product was neutralized with a 5% NaOH solution and then washed with saturated brine and distilled water. After that, the organic phase was distilled under reduced pressure to remove dichloromethane. The objective product was isolated by column chromatography (ethyl ether/ethyl acetate = 3:1).

The compound tetrahydroperfluorooctanol *m*-acryloyloxybenzoate (FMB or **5b**) was prepared under the same conditions used for FPB by the reaction of **3b** with acryloyl chloride.

Synthesis of FIP (5c). Compound 5-hydroxyisophthalic acid bis(tetrahydroperfluorooctanol) ester (**3c**) was prepared under the same conditions used for **3a** by the reaction of 5-hydroxyisophthalic acid with 1,1,2,2-tetrahydroperfluorooctanol.

Compound FIP (**5c**; route A) were prepared under the same conditions used for FPB by the reaction of **3c** with acryloyl chloride.

Synthesis of 5-acryloyloxyisophthalic acid (3d).^{21,22} 5-Hydroxyisophthalic acid (18.21 g, 0.10 mol) was neutralized with an equivalent NaOH solution, and then the mixture was placed into a flask. Acryloyl chloride (10.86 g, 0.12 mol) was added

dropwise within 2 h at 0°C and stirred at room temperature for an additional 12 h. Carbon tetrachloride was used as the solution. Finally, the mixture was adjusted to acid with dilute hydrochloric acid and subsequently washed with water and hot water. After drying, **3d** was obtained.

Synthesis of 5-acryloyloxyisophthaloyl dichloride. 5-Acryloyloxyisophthaloyl dichloride was prepared from **3d** and thionyl chloride with dimethylformamide as the catalyst. A mixture of **3d** (23.62 g, 0.10 mol), thionyl chloride (47.58 g, 0.40 mol), and dimethylformamide (0.50 mL) was added in a three-necked flask equipped with a magnetic stirrer and a reflux condenser. The reaction solution was kept at 60°C for 5 h. The resulting product was distilled under reduced pressure to remove the thionyl chloride. Finally, 5-acryloyloxyisophthaloyl dichloride was obtained as a colorless flaky crystal with a 95% yield.

Synthesis of 5c (FIP; route B). 5-Acryloyloxyisophthaloyl dichloride (27.31 g, 0.10 mol) and dichloromethane (50 mL) were introduced into a three-necked flask. 1,1,2,2-tetrahydroperfluoro-1-octanol (72.82 g, 0.20 mol) and TEA (20.24 g, 0.20 mol) were added dropwise within 2 h at 0°C and stirred at room temperature for an additional 12 h. The resulting mixture was subsequently washed with brine, a 5% NaOH solution, brine, and distilled water, respectively. Next, the organic phase was distilled under reduced pressure to remove the dichloromethane. The objective product was isolated by column chromatography (ethyl ether/ethyl acetate = 3:1).

Polymerization

Emulsion copolymerization was carried out as outlined in Scheme 3. A mixture of MMA, soft monomer (BA), fluorinated monomer (**5a**), Span-80, and sodium lauryl sulfate was pre-emulsified on an emulsification instrument. The mass ratio of MMA and BA was 1:3. The flask was stirred and heated to 70°C under a nitrogen atmosphere. A solution of potassium persulfate dissolved in distilled water was then dripped into the mixture within 1 h. The polymerization was kept for 3 h at a temperature of 70°C. Finally, the copolymer emulsion FPB/BA/

MMA (FPBB or **7a**) was obtained. The copolymers FPB/OA/MMA (FPBO or **8a**), FPB/DA/MMA (FPBD or **9a**), FMB/BA/MMA (FMBB or **7b**), FMB/OA/MMA (FMBO or **8b**), FMB/DA/MMA (FMBD or **9b**), FIP/BA/MMA (FIPB or **7c**), FIP/OA/MMA (FIPO or **8c**), and FIP/DA/MMA (FIPD or **9c**) were prepared with the same method.

Treatment of the Cotton Fabrics with Fluorinate Copolymers

The desized, scoured, bleached twill-weave cotton 133*72 2/1 weighed 128 (g/m²) fabric samples were immersed in an emulsion of obtained copolymers and then padded through two dips and two nips with a wet pickup of 95–100%. Finally, the samples were dried at 110°C for 3 min and cured at 170°C for 180 s.

We held the hypothesis that the density of the side chains (number of side chains per constitutional repeat unit) also played a profound role in determining the wetting characteristics of the aromatic fluorinated copolymers and corresponding fabrics.

RESULTS AND DISCUSSION

Preparation and Characterization of the Monomer

The esterification of tetrahydroperfluorooctanol with carboxylic acid could be described as nucleophilic substitution. For the strong electron-withdrawing effect of CF groups upon the —OH groups, the esterification of tetrahydroperfluorooctanol was difficult. The structure of carboxylic acid had great effects on both the reaction rate and the yield. For the aromatic carboxylic acids, the conjugated system increased the electron density of the carboxyl groups. In addition to the electronic effect, the steric effect also played an important role in determining the reaction ability. When the substituent was located in the phenyl ring, the esterification ability was lowered, and this was more obvious for metaposition; particularly, when two carboxylic groups were located in the metaposition of the phenyl ring, the esterification of both the carboxylic groups was difficult.

Monomer **5c** could be prepared by the same route as **5a** and **5b**, whereas the yield of the intermediate (**3b**) was relatively low. To prepare compound **5c** in higher yield, another synthesis route was designed.

Compound 3a. Colorless flaky crystal, 85% yield, mp = 116–118°C. FTIR (KBr, ν): 3394.5, 1699.3, 1614.5, 1591.1, 1513.6, 1358.5, 1297.1, 1226.9, 1165.5, 1126.0, 1095.3, 1048.5, 949.0, 885.4, 763.3, 739.8, 638.9.

Compound 3b. Colorless solid, 70% yield, mp = 68–70°C. FTIR (KBr, ν): 3425.2, 1706.6, 1598.4, 1466.8, 1336.1, 1281.0, 1219.6, 1158.2, 1111.4, 1048.5, 1003.1, 949.0, 832.0, 754.5, 709.1. ¹H-NMR (CDCl₃, 400 MHz, δ , ppm): 7.599 (d, J = 7.6 Hz, 1 H), 7.505 (m, 1 H), 7.320 (t, J = 8.0 Hz, 1 H), 7.064 (d, J = 8.0 Hz, 1 H), 5.279 (m, 1 H), 4.583 (t, J = 7.6 Hz, 2 H), 2.657 (t, J = 7.6 Hz, 2 H).

Compound 3c. Colorless small needle crystal, 25% yield, mp = 127–128°C. FTIR (KBr, ν): 3472.0, 1730.0, 1713.9, 1614.5, 1459.5, 1343.9, 1281.1, 1219.6, 1158.2, 1102.6, 1048.5, 1010.4, 963.6, 824.7, 763.3, 732.6. ¹H-NMR (CDCl₃, 300 MHz, δ , ppm): 8.240 (m, 1 H), 7.715 (m, 2 H), 5.356 (m, 1 H), 4.625 (m, 4 H), 2.693 (m, 4H).

Compound 5a. White solid, 90% yield. FTIR (KBr, ν): 2992.3, 1730.0, 1637.9, 1598.4, 1506.3, 1466.8, 1412.7, 1351.2, 1273.7,

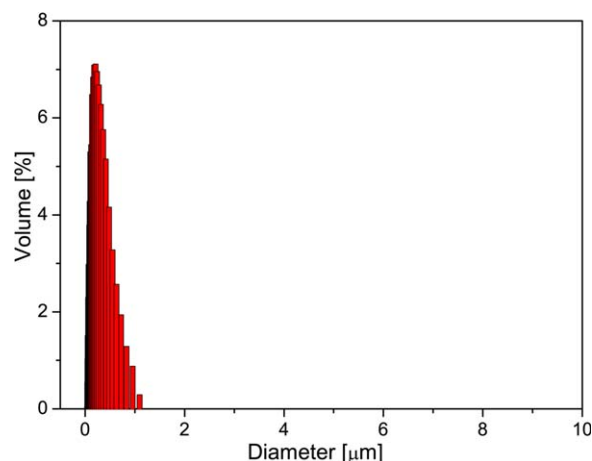


Figure 1. Particle size distribution of latex. [Color figure can be viewed in the online issue, which is available at wileyonlinelibrary.com.]

1243.0, 1203.5, 1158.2, 1102.6, 1048.5, 972.4, 855.4, 808.6, 770.6, 732.5, 700.4, 655.0. ¹H-NMR (CDCl₃, 400 MHz, δ): 8.083 (d, J = 8.8 Hz, 2 H), 7.241 (d, J = 8.8 Hz, 2 H), 6.628 (d, J = 17.2 Hz, 1 H), 6.322 (dd, J = 10.4 Hz, 17.2 Hz, 1 H), 6.044 (d, J = 10.4 Hz, 1 H), 4.607 (t, J = 7.6 Hz, 2 H), 2.684 (t, J = 7.6 Hz, 2 H).

Compound 5b. Oil, 85% yield. FTIR (KBr, ν): 2993.5, 1730.1, 1637.9, 1591.1, 1452.1, 1412.7, 1335.1, 1273.7, 1234.2, 1149.4, 1102.6, 987.0, 832.0, 801.3, 754.5, 700.4. ¹H-NMR (CDCl₃, 400 MHz, δ): 7.919 (d, J = 8.0 Hz, 1 H), 7.788 (m, 1 H), 7.479 (m, 1 H), 7.375 (m, 1 H), 6.624 (d, J = 10.8 Hz, 1 H), 6.325 (dd, J = 10.4 Hz, 17.2 Hz, 1 H), 6.043 (d, J = 10.8 Hz, 1 H), 4.589 (t, J = 7.6 Hz, 2 H), 2.661 (t, J = 7.6 Hz, 2 H).

Compound 3d. White powder, 90% yield. FTIR (KBr, ν): 3556.9, 3454.2, 3091.9, 2592.8, 2533.7, 1764.1, 1722.1, 1670.8, 1611.7, 1476.4, 1409.5, 1316.3, 1257.2, 1215.2, 1163.9, 994.4, 910.5, 800.1, 758.1, 681.9. ¹H-NMR (DMSO, 400 MHz, δ): 14.842–12.245 (m, 2 H), 8.368 (m, 1 H), 7.942 (m, 2 H), 6.583 (d, J = 17.2 Hz, 1 H), 6.428 (dd, J = 10.4 Hz, 17.2 Hz, 1 H), 6.190 (d, J = 10.0 Hz, 1 H).

Compound 5c. Colorless solid, 88% yield (route A), 85% yield (route B). FTIR (KBr, ν): 1739.2, 1638.2, 1594.6, 1468.7, 1409.6, 1324.1, 1223.0, 1146.8, 1104.8, 1037.9, 961.8, 826.5, 733.2, 699.0. ¹H-NMR (CDCl₃, 300 MHz, δ): 8.557 (m, 1 H), 8.027 (m, 2 H), 6.672 (d, J = 17.1 Hz, 1 H), 6.351 (dd, J = 10.5 Hz, 17.1 Hz, 1 H), 6.107 (d, J = 9.9 Hz, 1 H), 4.637 (m, 4 H), 2.694 (m, 4 H).

Microstructure of the Copolymers

Particle Size of the Latexes. The particle size is an index of the quality and the stability of the emulsion. The dispersion particle size was measured by a laser particle size analyzer, which worked with principle of Mie scattering to precisely determine the particle size distribution. The particle size distribution by the volume content (%) of the different sizes of particles in the fluorinated latexes is shown in Figure 1. The average size of the latex particles was 0.15–0.20 μm , 90% of which distributed between 0.09 and 0.50 μm . The results indicated that the

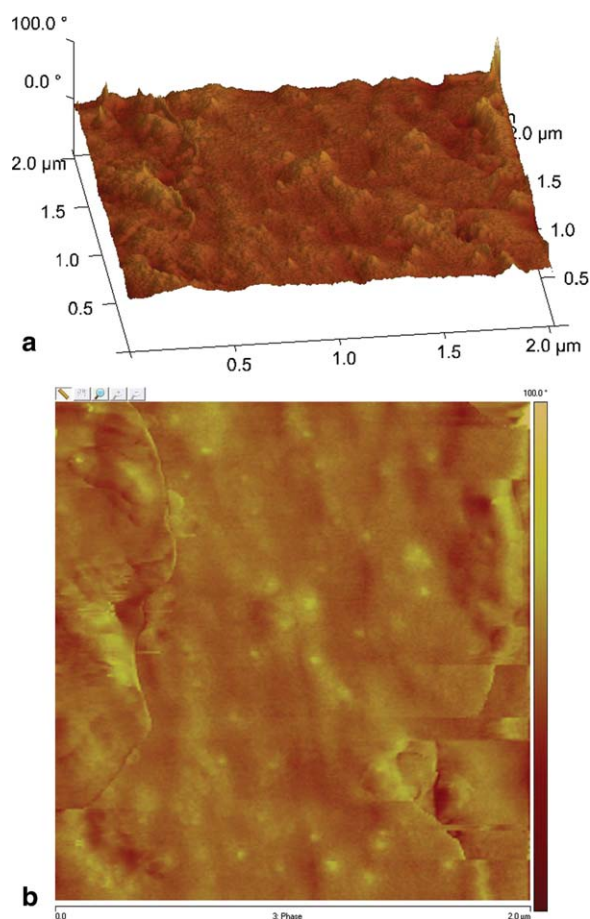


Figure 2. AFM image of the cotton surface treated with FIPB: (a) height and (b) phase. [Color figure can be viewed in the online issue, which is available at wileyonlinelibrary.com.]

emulsion particle size distribution was uniform, and the emulsion was stable.

Surface Morphology of the Treated Cotton. Microscale roughness of the outmost surface has been thought to be an effect of the generation of superhydrophobic properties.^{23–25} AFM measurement was performed to investigate the surface morphology of the treated cotton. The microstructure of the FIPB-coated cotton surface (Figure 2) showed many protruding nodes distributed in the surface. Because of the strong electrophilic addition and low steric hindrance of fluorine atoms in the side perfluoroalkyl (Rf) groups, the fluorine groups had a relatively low surface energy. During the curing process, the fluorinated segments aggregated and sprayed out; this resulted in the formation of protruding nodes distributed in the surface.

WAXD of the Copolymer Films. It is well known that the crystallization of poly(fluoroalkyl acrylate)s depends on side Rf groups. Poly(fluoroalkyl acrylate)s with long Rf groups showed more of a tendency to crystallize at room temperature, whereas poly(fluoroalkyl acrylate)s with short Rf groups were mostly found to be in an amorphous state. The crystallization information of FPBB, FMBB, and FIPB was further investigated with WAXD. Except for some small diffraction peaks in the curves (Figure 3), no obvious diffraction peak was observed in the

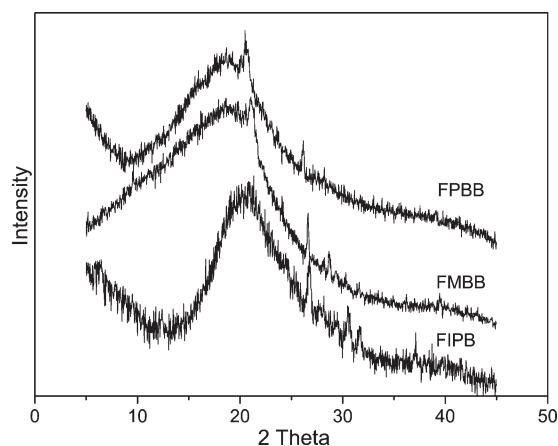


Figure 3. WAXD curves of the copolymers.

WAXD spectrum of the fluorinated copolymers. This confirmed that the fluorinated copolymers were mainly distributed in an amorphous order; meanwhile, some of the fluorinated groups aggregated and caused microphase separation in the internal structure.

Chemical Composition of the Copolymers

FTIR Analysis. The chemical structures and compositions of the copolymers (FPBB, FMBB, and FIPB) were investigated by FTIR spectroscopy (Figure 4). The spectra of the polymers showed strong C–F absorption bands at 1100–1300 cm^{-1} . The stretching vibration absorption of 1100–1240 cm^{-1} overlapped with the stretching vibration absorption of the ester groups at 1250 cm^{-1} , and the absorption at 1288 cm^{-1} was attributed to CF_3 groups. The unambiguous disappearance of the characteristic peak of C=C at 1639 cm^{-1} was observed. This indicated the completion of the polymerization. An intense absorption band at 1730–1760 cm^{-1} arose from the C=O stretching modes. The characteristic stretching peaks of C–H were evident at 2850–3000 cm^{-1} .

$^1\text{H-NMR}$ Analysis. Figure 5 shows the typical $^1\text{H-NMR}$ spectrum of FIPB. The typical peaks of CH in the aromatic ring emerged around 8.0 ppm. The O–CH₃ peak in MMA and O–CH₂ peak of BA were observed at 3.6 and 4.1 ppm,

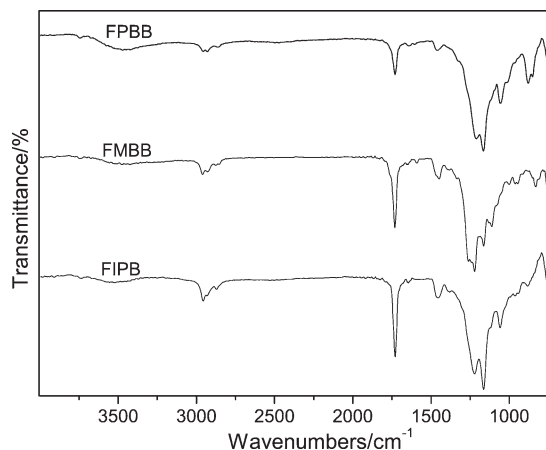


Figure 4. FTIR spectra of the copolymer films.

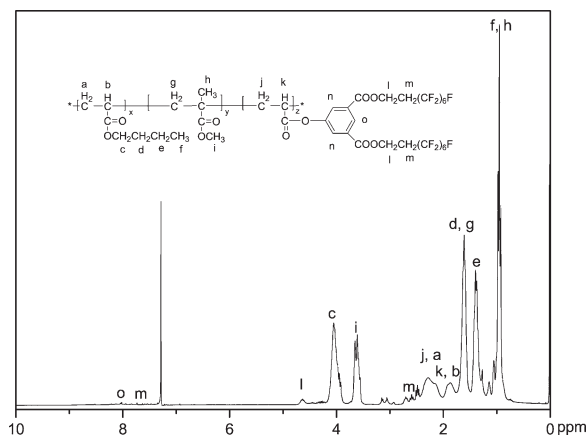


Figure 5. ¹H-NMR of the copolymer FIPB.

respectively. The O—CH₂ and CH₂CF₂ peaks in FIP were found at 4.3 and 2.5 ppm, respectively. According to the FTIR and ¹H-NMR results, the formation of the fluorinated copolymer could be confirmed.

Surface Chemical Composition of the Cotton Fabrics Treated with Copolymers. The surface properties of the copolymers were significantly affected by the surface composition and structure in the multicomponent copolymer systems. The surface compositions of the cotton fabrics treated with copolymers

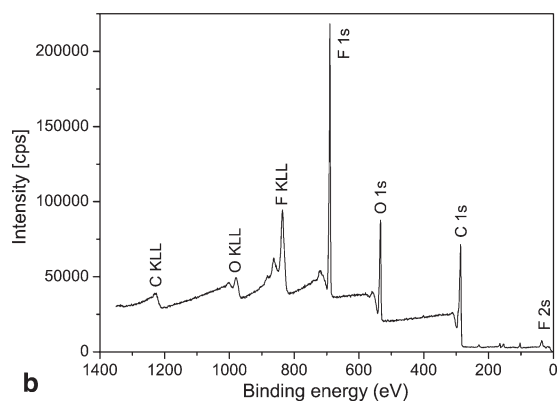
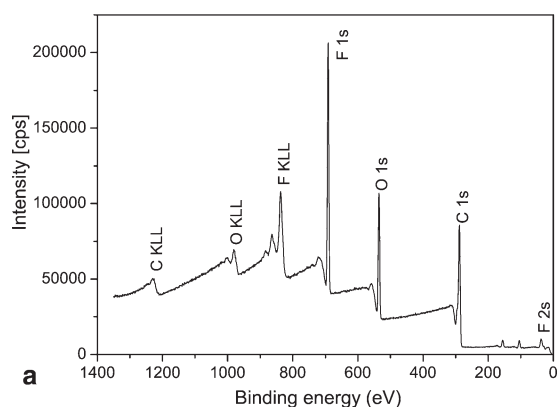


Figure 6. Wide-scan survey spectrum of the cotton fabrics surfaces (a) treated with FMBB and (b) treated with FIPB. KLL, Auger spectra of corresponding element.

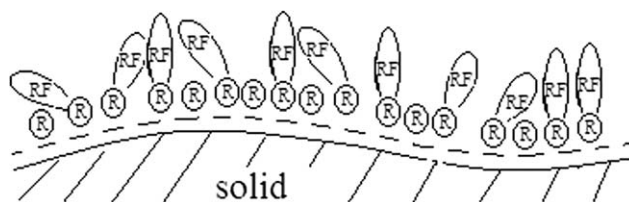


Figure 7. Schematic drawing of the postulated surface ordering.

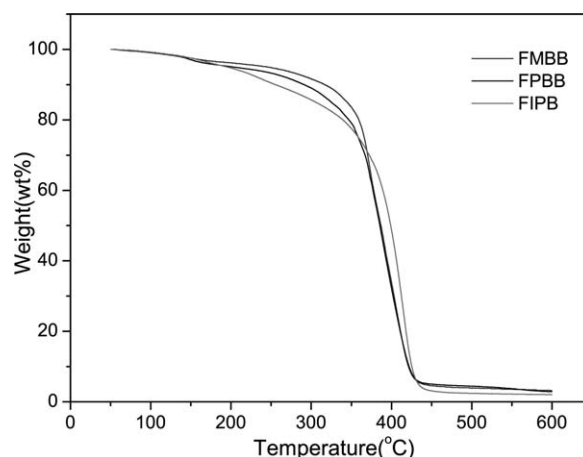


Figure 8. TG curves of the copolymers.

FMBB and FIPB were investigated by XPS measurements. The results of carbon, fluorine, and oxygen atomic compositions for the copolymers are given in Figure 6. The XPS spectra of the constituent elements revealed carbon, fluorine, and oxygen as the main elements. From the results, we reflected that the out-most surface of the fluorinated copolymers mainly consisted of Rf groups; meanwhile, some of the ester groups and aliphatic groups were directly exposed to the air side at the copolymer–air interface. To explain these results simultaneously, the out-most surface layer must have had a structure similar to an irregular arrangement of Rf groups where some of the ester groups and aliphatic groups were directly exposed to the air side. A schematic drawing of the surface ordering postulated is shown in Figure 7, wherein, RF represented fluorinated segment and R

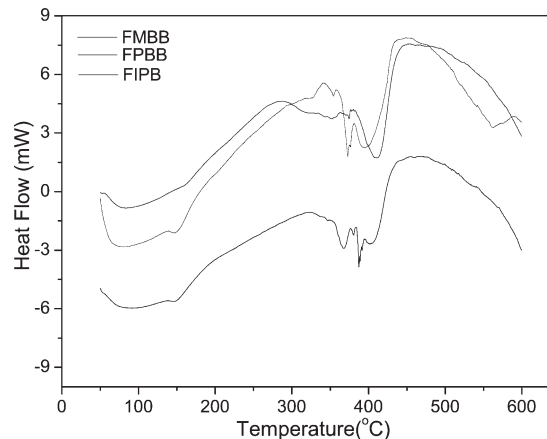


Figure 9. DTA curves of the copolymers.

Table I. Thermal Degradation Characteristics of the Fluorinated Copolymers

Copolymer	TG curve			DTA curve			
	IDT (°C)	T_{\max} values (°C)	Δm (%)	Peak temperature (°C)	Thermal effect	Peak temperatures (°C)	Thermal effect
FMBB	318	371, 390, 407	96.80	86	Endothermic	366, 403	Endothermic
FPBB	302	390	97.12	81	Endothermic	370, 395	Endothermic
FIPB	322	413	97.95	71	Endothermic	355, 410	Endothermic

T_{\max} , temperature corresponding to the temperature where the decomposition rate was maximum; Δm , weight loss at 600°C.

represented fluorine-free groups. The percentage of fluorine was calculated from the peak strength of F1s. The calculated atomic concentration of F in the outermost surface coated with FIPB was 34.5%; this was significantly higher than the atomic concentration in the bulk of FIPB (F, 16%). The fluorine concentration in the outermost surface of the cotton fabric treated with FMBB was also investigated and was found to be 29.8%. The higher fluorine concentration in the outermost surface of FIPB also indicated more regularity in the fluorinated chains. We expected that the more the regularity of the arrangement of Rf groups increased, the more its surface properties were enhanced.

Properties of the Copolymers

Thermal Properties. Heat treatment is usually carried out during the finishing and wearing processes and include curing and ironing. Therefore, thermal stability is very important for fluorinated copolymers that are used to treat cotton fabrics; oxidation decomposition should be avoided in heat treatment. The thermal degradation behaviors of the fluorinated copolymers were studied with thermogravimetric analysis (Figure 8) and DTA (Figure 9) at a heating rate of 10°C/min in a nitrogen atmosphere, and the results are summarized in Table I.

The tiny endothermic peaks around 80°C accompanied by microscopic weight loss resulted from the removal of water and the residual nonaqueous solvent. It could be seen that the initial decomposition temperature (IDT; 5% weight loss) for FMBB and FIPB were 244 and 195°C, respectively. The difference might have been derived from the introduction of two functional groups ($-\text{OCH}_2\text{CH}_2\text{C}_6\text{F}_{13}$) to the FIP molecule. It is well known that the bond energy of the ether bond is lower than

that of the carbon–carbon bond, so the introduction of the functional group would have affected the thermal stability of the FIPB polymer. However, the temperature corresponding to the maximum rate of degradation for FIPB (411°C) was higher than that of FMBB (372°C). The emergence of the obvious endothermic peaks in the range 300–400°C indicated the oxidation thermal cracking of the copolymers; this was well in accordance with the trend of the TG curves.

Surface Properties of the Fluorinated Copolymers. The surface energies of the fluorinated polymer were evaluated with the Owens concept. By measuring the contact angles formed on the solid surface with water and hexadecane, we calculated the surface free energy of the solid. The surface tension (γ_1) and the dispersion ($^d\gamma_1$) and polar ($^p\gamma_1$) components of the surface tension for water ($\gamma_1 = 72.8$ mN/m, $^d\gamma_1 = 21.8$ mN/m, and $^p\gamma_1 = 51.0$ mN/m) and hexadecane ($\gamma_1 = 27.6$ mN/m, $^d\gamma_1 = 27.6$ mN/m, and $^p\gamma_1 = 0$ mN/m) were used to calculate the surface energies of the modified surfaces. The results are shown in Table II. The surface energy of a solid can be resolved into dispersion and polar components. According to the polar and dispersion components of the surface energy, the dispersion component had a significant contribution compared to the polar component, but the polar component was not negligible. In the molecule of the fluorinated copolymers, the ester group of $-\text{COO}-$ was more polar than the other groups (aliphatic groups, aromatic nucleus, and fluorine groups). When the polar liquid was placed on the surface, we deduced that there might have existed a hydrogen-bonding interaction that was much more significant than that with the surface fluorine groups. The hydrogen-bonding interaction between ester groups with water was likely to be much more important than that of others. The existence of ester groups at the copolymer–air interface could have given a strong hydrogen-bonding interaction with the polar liquid. Because the surface energy reflected mainly the chemical composition of the outermost surface, it was possible to infer that some of the ester groups of the fluorinated copolymers might have been exposed to the copolymer–air interface. This was in good accordance with the XPS results. The tendency toward aggregation and self-alignment of the Rf groups were important in the control of their surface properties.²⁶ The adjacent groups might have been beneficial to the aggregation and self-alignment of the Rf groups on the polymer surface. The surface energy value of the copolymer FIPB was considerably lower than that of FMBB and FPBB.

The water and oil repellency of the treated cotton fabrics was examined. Contact angle measurement was used to study the

Table II. Contact Angles and Surface Energies of the Fluorinated Copolymers

Sample	Water contact angle (°)	Hexadecane contact angle (°)	γ_S (mN/m)	γ_S^d (mN/m)	γ_S^p (mN/m)
Glass	Spread out	Spread out	—	—	—
FPBB	112.3	74.3	12.10	11.14	0.96
FMBB	114.0	76.0	11.42	10.64	0.79
FIPB	116.6	85.6	9.18	8.00	1.18
FIPO	119.8	93.1	7.05	6.17	0.88

γ_S , surface free energy; γ_S^d , dispersion component of the surface free energy; γ_S^p , polar dispersion component of the surface free energy.

Table III. Water and Oil Repellencies of the Cotton Fabrics Coated with Fluorinate Copolymers

Sample	Functional monomer	Soft monomer	Water contact angle (°)	Water-repellency rate	Oil-repellency rate
Untreated	—	—	0	0	0
FPBB	FPB	BA	133	7	2
FPBO	FPB	OA	136	7	1.5
FPBD	FPB	DA	137	7	2
FMBB	FMB	BA	135	7	2
FMBO	FMB	OA	137	7	1.5
FMBD	FMB	DA	139	7.5	2.5
FIPB	FIP	BA	138	8	3
FIPO	FIP	OA	141	8	5
FIPD	FIP	DA	137	8	3

water-repellent properties of the finished textile, and the drop test was also used to further investigate the waterproofing properties. The results are summarized in Table III. Among all of the cotton fabrics treated with FIP copolymers, the cotton-fabric-treated FIPO showed the highest water and oil repellencies. The results reflect that OA had a better synergetic effect with FIP and resulted in a lower surface free energy of the homologous fluorinated polyacrylate. The fabrics treated with the FPB copolymer showed similar water and oil repellencies to that of the FMB copolymer. The FIP copolymers contained two adjacent, short fluorinate esters segments, and they provided better water and oil repellencies than the corresponding FMB and FPB copolymers. The better water and oil repellencies of the FIP copolymers might have been due to the higher concentration of F in the outermost surface of the FIP copolymers. It also reflected that the enrichment of fluorine segments on the surface played an important role in achieving high water and oil repellencies.

CONCLUSIONS

Three aromatic monomers containing one or two fluoroalkyl groups were synthesized and characterized. The novel fluorinated monomers were copolymerized with acrylate and MMA by conventional emulsion polymerization. The copolymer emulsions were used to treat cotton fabrics. The relationships between the structure and properties of the copolymers were investigated. We observed that the aromatic copolymers containing two adjacent fluorinated segments showed higher fluorine concentrations in the outermost surface and exhibited better water and oil repellencies than the monofluorinated aromatic copolymers. The behaviors, together with the surface energy, further supported the hypothesis that the density of side chains (number of side chains per constitutional repeat unit) played a profound role in determining the wetting characteristics of the fluorinated copolymers.

ACKNOWLEDGMENTS

The financial support of the National Natural Science Foundation of China (contract grant numbers 51273140 and 51273134), a Pro-

ject Funded by the Priority Academic Program Development of Jiangsu Higher Education Institutions, and the Program Sponsored for Scientific Innovation Research of College Graduate in Jiangsu Province (contract grant number CXZZ11-0106) is greatly appreciated.

REFERENCES

1. Li, K.; Wu, P. P.; Han, Z. W. *Polymer* **2002**, *43*, 4079.
2. Lim, H.; Lee, Y.; Park, I. J.; Lee, S. B. *J. Colloid Interface Sci.* **2001**, *241*, 269.
3. Saidi, S.; Guittard, F.; Guimon, C.; Geribaldi, S. *Eur. Polym. J.* **2006**, *42*, 702.
4. Timperley, C. M.; Arbon, R. E.; Bird, M.; Brewer, S. A.; Parry, M. W.; Sellers, D. J.; Willis, C. R. *J. Fluorine Chem.* **2003**, *121*, 23.
5. Giesy, J. P.; Kannan, K. *Environ. Sci. Technol.* **2001**, *35*, 1339.
6. Ellis, D. A.; Martin, J. W.; Silva, A. O. D.; Mabury, S. A.; Hurley, M. D.; Anderson, M. P. S.; Wallington, T. J. *Environ. Sci. Technol.* **2004**, *38*, 3316.
7. Renner, R. *Environ. Sci. Technol.* **2005**, *39*, 56A.
8. Xu, S. P.; Liu, W. Q. *J. Fluorine Chem.* **2008**, *129*, 125.
9. Chen, L. J.; Shi, H. X.; Hu, H. K.; Xiang, J. P. *J. Fluorine Chem.* **2010**, *131*, 731.
10. Ren, Q. Q.; Zhao, T. *Carbohydr. Polym.* **2010**, *80*, 381.
11. Pittman, A. G.; Ludwig, B. A. *J. Polym. Sci.* **1969**, *A7*, 3053.
12. Cassidy, P. E.; Aminabhavi, T. M.; Flarley, T. M. *J. Macromol. Sci. Part C: Rev. Macromol. Chem. Phys.* **1989**, *29*, 365.
13. Reddy, V. S.; Weikel, W. J.; Arbaugh, J.; Fitch, J. W.; Cassidy, P. E.; Clair, A. K. S. *Polymer* **1996**, *37*, 4653.
14. Ye, H. H.; Li, Z. X.; Chen, G. Q.; Fan, D. *J. Appl. Polym. Sci.* **2013**, *127*, 402.
15. Utsumi, Y.; Dazai, T. U.S. Pat. 0,022,911 (2013).
16. Hoshino, T. U.S. Pat. 0,184,695 (2012).
17. Cui, X. J.; Zhong, S. L.; Wang, H. Y. *Colloids Surf. A* **2007**, *303*, 173.

18. Xu, S. P.; Liu, W. Q. *J. Fluorine Chem.* **2008**, *129*, 125.
19. Tamai, T.; Watanabe, M.; Maeda, H.; Mizuno, K. *J. Polym. Sci. Part A: Polym. Chem.* **2008**, *46*, 1470.
20. Tronc, F.; Li, M.; Lu, J.; Winnik, M. A.; Kaul, B. L.; Graciet, J. *J. Polym. Sci. Part A: Polym. Chem.* **2003**, *41*, 766.
21. Sessa Sainath, A. V.; Kameswara Rao, A.; Rami Reddy, A. V. *J. Appl. Polym. Sci.* **2000**, *75*, 465.
22. Zhang, B. Y.; Hu, J. S.; Zang, B. L.; Zhou, A. J. *J. Appl. Polym. Sci.* **2003**, *88*, 1936.
23. Woodward, I.; Schofield, W. C. E.; Roucoules, V.; Badyal, J. P. S. *Langmuir* **2003**, *19*, 3432.
24. Hsieha, C. T.; Chena, J. M.; Kuo, R. R.; Lin, T. S.; Wu, C. F. *Appl. Surf. Sci.* **2005**, *240*, 318.
25. Ivanova, N. A.; Zaretskaya, A. K. *Appl. Surf. Sci.* **2010**, *257*, 1800.
26. Chiba, K.; Kurogi, K.; Monde, K.; Hashimoto, M.; Yoshida, M.; Mayama, H.; Tsujii, K. *Colloids Surf. A* **2010**, *354*, 234.